Journal of New Materials for Electrochemical Systems 16, 083-087 (2013)
© J. New Mat. Electrochem. Systems

Facile Synthesis of Donut-like TiO_2-SnO_2 Nanocomposite Microspheres by a Two-step Hydrothermal Reaction and Subsequent Spray Drying Process and Its Electrochemical Lithium Storage Properties

Mengyao Tian, Chunju Lv*, Jie Xu, Bing Guo, Da Chen and Kangying Shu

College of Materials Science and Engineering, China Jiliang University, Hangzhou 310018, PR China

Received: December 25, 2012, Accepted: February 04, 2013, Available online: April 03, 2013

Abstract: *Donut-like TiO_2-SnO_2 nanocomposite microspheres were successfully synthesized via a facile two-step hydrothermal reaction and subsequent spray drying. The protonated titanate nanowires with $H_2Ti_3O_7$ phase in the nanocomposite precursor transformed into not anatase TiO_2 but TiO_2(B) crystal structure even after calcination at 400 ℃. And the substitutional solid solution (Sn, Ti)O_2 with the same tetragonal rutile structure as SnO_2 was formed. Moreover, the hierarchical donut-like structure in TiO_2-SnO_2 nanocomposite microspheres constructed by the second-step hydrothermal and spray drying treatment was maintained after calcination at 400 ℃. The electrochemical test showed that the as-obtained TiO_2-SnO_2 nanocomposite microspheres reached an initial discharge capacity of 640 m Ah g^{-1} at a current density of 40 mA.g^{-1}, which is much higher than the theoretical capacity of TiO_2(B).*

Keywords: TiO_2-SnO_2 nanocomposite; hydrothermal reaction; spray drying; electrochemical performance

1. INTRODUCTION

Recently, there has been considerable interest in metal oxide as a potential anode material for use in lithium ion batteries [1]. Among them, TiO_2 especially the one with anatase crystal structure is extensively studied because it is abundant, environmentally benign and delivers a high discharge voltage plateau of about 1.7 V, stable cycling performance, and small volume expansion (~3%) during lithiation/delithiation [2-5]. Besides anatase TiO_2, the other polymorphs like rutile, brookite and TiO_2(B) have been demonstrated to possess the lithium storage properties [6-12]. Their theoretical specific capacity of TiO_2 is estimated to be less than 335 mAh g^{-1} which is lower than that of the commercial graphite at 372 mAh g^{-1}, so low capacity (200 mAh g^{-1}) was usually observed. When they were prepared as nanostructure forms (e.g. nanowires, nanotubes, nanowhisker or nanosheet), higher capacity from 200 to 300 mAh g^{-1} was achieved [7, 10, 13-15]. However, the high capacity above 200 mAh g^{-1} was hard to maintain after long cycles due to their structural instability, which can be one of the shortcomings of their anode application [16-19].

SnO_2 is another extensively investigated anode material with a high theoretical lithium storage capacity (790 mAh g^{-1}). However, it experiences a strong volume change (up to 300 vol.%) during its alloying reaction with lithium ion, which leads to mechanical stress and loss of contact to the current collector and thus to strong capacity fading [20-22]. In order to overcome these obstacles, the preparation of nanostructured SnO_2 morphologies has been pursued and the capacity is better retained because of their large strain accommodation ability, short diffusion distance and thus rapid Li^+ insertion/de-insertion in the small grains [22, 23]. On the other hand, constructing nanocomposite architectures is demonstrated to be able to further improve the Li^+ storage capacity and cycle stability of SnO_2 materials due to the "buffering" and "mechanical support" functions from the matrix materials during charge–discharge cycling [24, 25]. Up to now, various TiO_2-supported-SnO_2 materials had been prepared and exhibited favorable electrochemical performances, which enabled the potential application of those materials in lithium ion batteries [26-31]. However, for the sake of their practical application, there still exist many challenges in synthesizing TiO_2-SnO_2 nanocomposite by facile synthesis routes.

Herein, considering the advantages of the TiO_2-B, which shows the largest specific capacity among the different TiO_2 polymorphs and can be obtained by a simple hydrothermal method, we first reported a facile synthesis of TiO_2-SnO_2 nanocomposite by a two-

*To whom correspondence should be addressed: Email: lvchunju@cjlu.edu.cn
Phone: + 86 571 86835738; Fax: + 86 571 86835740

step hydrothermal reaction and subsequent spray drying process. The characteristics of the as-prepared nanocomposite and the electrochemical performances as a lithium intercalation host were investigated.

2. EXPERIMENTAL

2.1. Synthesis of TiO_2-SnO_2 nanocomposite

TiO_2-SnO_2 nanocomposite was prepared via a two-step hydrothermal reaction and subsequent spray drying route. Titanate nanowires were firstly obtained, which was commonly referred in the previous literatures [9, 10, 12]. TiO_2 powders (Degussa P25, ca. 80% anatase, 20% rutile) were used as received. All other chemicals were of analytical reagent grade and used without further purification. Deionized water was used throughout. In a typical synthesis process, commercial P25 powders of 1.0 g were added into the aqueous NaOH solution (60 mL, 10 mol.L^{-1}). After stirring for 1 h, the resulting suspension was transferred into a Teflon-lined stainless steel autoclave (100 mL). The autoclave was maintained at 180 ℃ for 12 h in oven and then naturally cooled to room temperature. The obtained precipitate was washed with HCl (0.1 mol.L^{-1}) solution and then with deionized water until pH≈7.0. Subsequently, the precipitate was dispersed into 40 mL water to form a white suspension by ultrasonication and subsequent stirring, followed by the addition of $SnCl_4 \cdot 5H_2O$ with the TiO_2/SnO_2 weight ratio of 55/45. Then, 20 mL NaOH solution (containing 4.3 g NaOH) was dropped into the above suspension. After stirring for 1 h, the resulting suspension was again treated at 200 ℃ for 12 h in the Teflon-lined stainless steel autoclave. After washing with water for 3 times, the obtained precipitate was dispersed into 120 mL water homogeneously with the assistance of ultrasound, followed by spray drying at the inlet and outlet temperature of 150 and 80 ℃ respectively to obtain the nanocomposite precursor. The spray-dried precursor was finally heated at 400℃ for 3 h in air in a covered alumina crucible at a heating rate of 2℃.min^{-1}, resulting in the TiO_2-SnO_2 nanocomposite. In comparison, pure TiO_2 was obtained by one-step hydrothermal reaction and post-heat treatment. And pure SnO_2 was also synthesized by one-step hydrothermal route at the same conditions without calcination.

2.2. Characterizations

The thermogravimetric analysis (TGA) was used to observe the decomposition reaction of the as-prepared precursor and determine the calcination temperature. The experiments were performed using a METTLER TOLEDO TGA/DSC 1LF1600 apparatus with the temperature from 30 to 600℃ at a heating rate of 5℃.min^{-1} under an air atmosphere. X-ray diffraction (XRD) measurements were carried out on a diffractometer (Bruker D2 PHASER) with Cu Kα radiation in the range from 10° to 90°. The morphology of the samples was studied with a scanning electron microscope (SEM, JEOL JEM-5610). The energy dispersive X-ray analysis was conducted using the EDX analyzer equipped with the TEM in point mode.

2.3. Electrochemical measurements

The working electrodes were prepared from the as-synthesized active nanocomposite, carbon black as a conducting agent, and poly(vinylidene difluoride) (PVDF) binder dissolved in *n*-methyl pyrolidinone(NMP, 8 wt%) at a weight ratio of 8:1:1. The slurry was mixed overnight to obtain a homogeneous black paste and then spread onto a copper foil current collector, followed by drying at 120℃ in vacuum for 12 h. Copper-foil pieces with 14mm diameter were then cut off and used as the electrode in homemade cells which were assembled inside Ar filled glove box. The average amount of TiO_2-SnO_2 nanocomposite in a round piece of electrode is about 5 mg. Each electrode was carefully weighted before use and several electrodes were tested to assume the reproducibility of the electrochemical behavior. The coin cells (CR 2015) also used Li metal as a counter electrode, a Celgard 2500 as a separator and a 1 M $LiPF_6$ dissolved in ethylene carbonate (EC), dimethyl carbonate (DMC), and ethylene methyl carbonate (EMC) (1:1:1, v/v/v) as an electrolyte.

The assembled cells were aged for 12 h before testing and then were galvanostatically charged and discharged over a voltage range of 2.5–0.01V vs. Li^+/Li at a current density of 40 mA g^{-1} using a LAND cell test (Land-CT 2001A) system. The specific capacity was calculated based on the mass of active materials in the electrode.

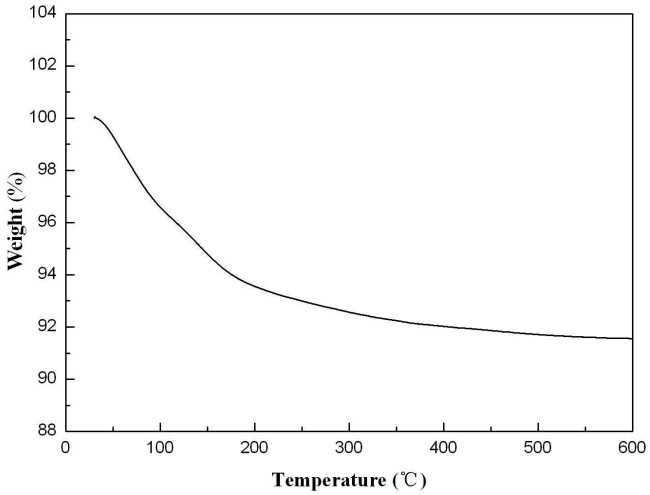

Figure 1. TGA profile of the spray-dried precursor for TiO_2-SnO_2 nanocomposite.

3. RESULTS AND DISCUSSION

The TGA profile of the spray-dried precursor for TiO_2-SnO_2 nanocomposite is shown in Fig. 1, revealing that the dehydration process of the precursor starts at about 60°C and is finished at about 400 ℃. The total weight loss recorded in this range for the nanocomposite precursor is about 8%, which is mainly attributed to the dehydration of the absorbed water, interlayer water and structural water in the resulting protonated titanate nanowires after hydrothermal treatment [32]. No significant weight loss was observed beyond 400°C. So the calcination temperature for the TiO_2-SnO_2 nanocomposite is set at 400°C in our experiment.

Fig.2 shows the XRD patterns of the as-prepared samples. The protonated titanate nanowires with $H_2Ti_3O_7$ phase were obtained and then transformed into TiO_2(B) (JCPDS 46-1237) after heating at 350℃ as clearly shown in the upper right inset, where the diffraction peaks of $H_2Ti_3O_7$ and TiO_2(B) are both broadened greatly due to their 1D structures [9, 32]. When the protonated titanate

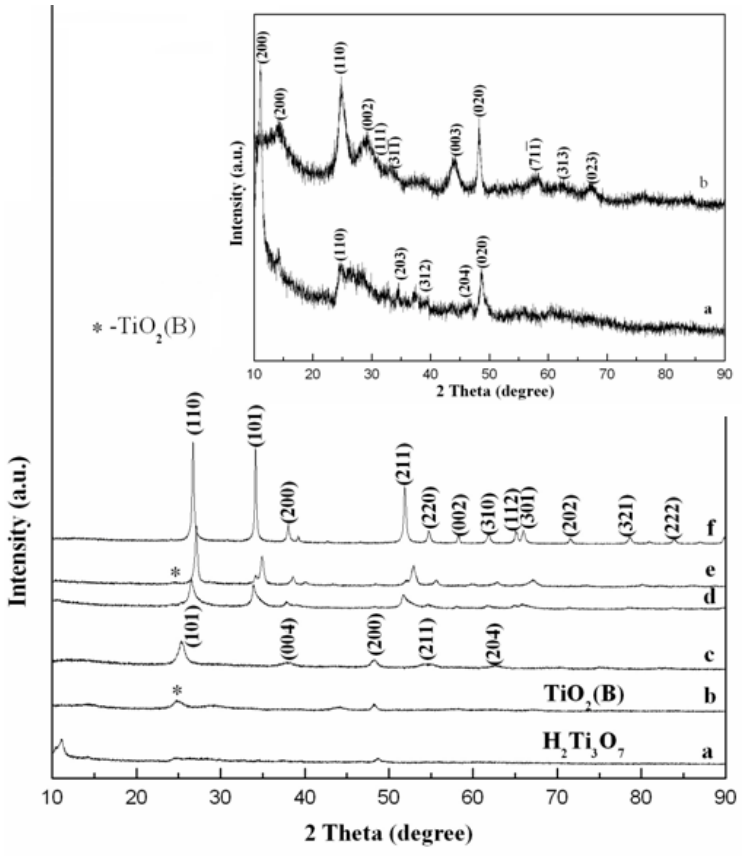

Figure 2. XRD patterns of samples: (a) pure precursor for TiO_2, (b) TiO_2 after calcination at 350°C, (c) TiO_2 after calcination at 400°C, (d) nanocomposite precursor for TiO_2-SnO_2, (e) TiO_2 -SnO_2 nanocomposite after calcination at 400°C, and (f) pure SnO_2. The upper right inset is the two XRD patterns of a and b for higher definition purpose.

nanowires were heated at 400℃ for 3h, the main phase is assigned as anatase TiO_2 (JCPDS 21-1272) with relatively strong diffraction intensities due to the increasing crystallinity (Fig.2c). Such results show that the pure protonated titanate nanowires transform into not TiO_2(B) but more thermodynamic stable anatase TiO_2 above 400℃. According to Fig.2f, pure SnO_2 with a tetragonal rutile structure (JCPDS 14-1445) can be prepared by one-step hydrothermal treatment. By a two-step hydrothermal reaction, the protonated titanate nanowires and SnO_2 are successively produced and form the nanocomposite precursor (Fig.2d). The average particle size of the SnO_2 in the nanocomposite was about 100 nm calculated from Sherrer equation. After calcination at 400 ℃, here we find that TiO_2 from the nanocomposite maintains the TiO_2(B) crystal structure, which will be beneficial for the lithium storage property. On the other hand, no obvious increase in the size of SnO_2 is observed (Fig.2e) as individual SnO_2 nanoparticles in the case of the TiO_2 nanowire matrix do not interact with each other during heating (shown in the SEM image below), which is very important for the values of capacity components and stability of lithium recharging. Another interesting phenomenon appearing in the TiO_2-SnO_2 nanocomposite is that all the XRD peaks ascribed to SnO_2 move to higher angles, indicating that Ti with smaller atom radius than that of Sn solubilizes in SnO_2 and the substitutional solid solution (Sn, Ti)O_2 with the slightly smaller lattice parameters is formed.

The morphology of the nanocomposite precursor was observed by field emission scanning electron microscopy in Fig. 3a. The product by a two-step hydrothermal reaction demonstrates a donut-like microsphere morphology with a size ranging from 1 μm to 5 μm. As clearly seen from the higher magnification SEM image inset in Fig.3a, the donut-like microsphere consists of protonated titanate nanowires and tiny SnO_2 nanoparticles. And the hierarchical donut-like microsphere structure is well retained after heat treatment at 400℃ (Fig.3b). Here, SnO_2 nanoparticles with a particle size about 100nm are individually wrapped by the TiO_2 nanowires which can serve as the buffering matrix for SnO_2 during Li^+ intercalation /deintercalation. Another phenomenon shown in the SEM images is that the surface of the donut particle becomes rougher and porous after the heat treatment. This may be ascribed to the TiO_2 transformation from TiO_2-B to more stable anatase TiO_2 phase and gradual collapse of its 1D structure at higher temperature. The porous morphology also may be from the formation of substitutional solid solution (Sn, Ti)O_2 with smaller lattice parameter which leads to the volume shrinkage in the nanocomposite.

Furthermore, the composition of this nanocomposite was also confirmed by the EDX spectroscopy experiments (Fig. 3c), which reveals the presence of Ti, Sn, O and Na in the nanocomposite. The amount of sodium residual from the raw NaOH stuff as determined by EDX analysis is only 5.3 wt%. The average Ti/Sn weight ratio

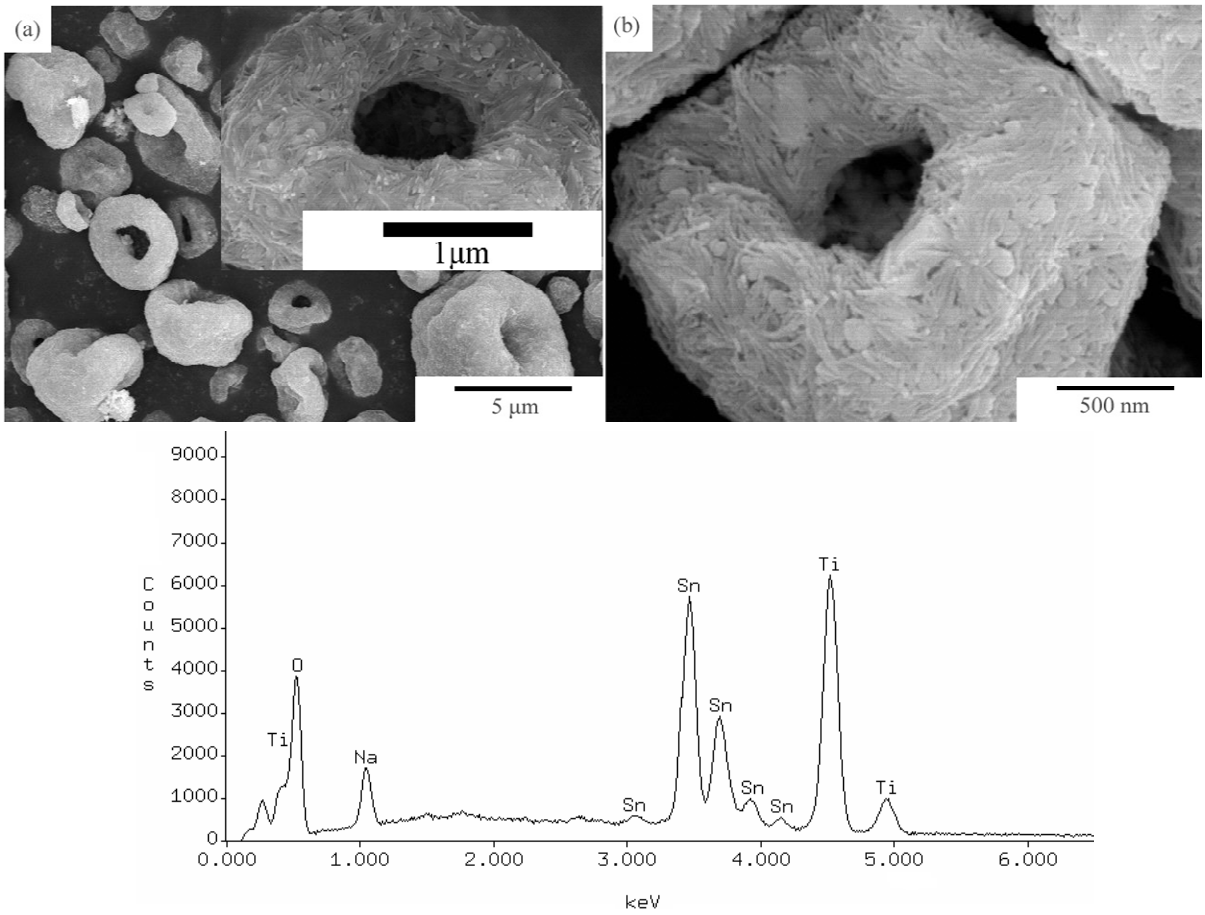

Figure 3. FESEM images of (a) the nanocomposite precursor, (b) TiO_2-SnO_2 nanocomposite after calcination at 400℃. (c) Typical EDX spectrum of the TiO_2-SnO_2 nanocomposite. The upper right inset in (a) is an enlarged SEM image.

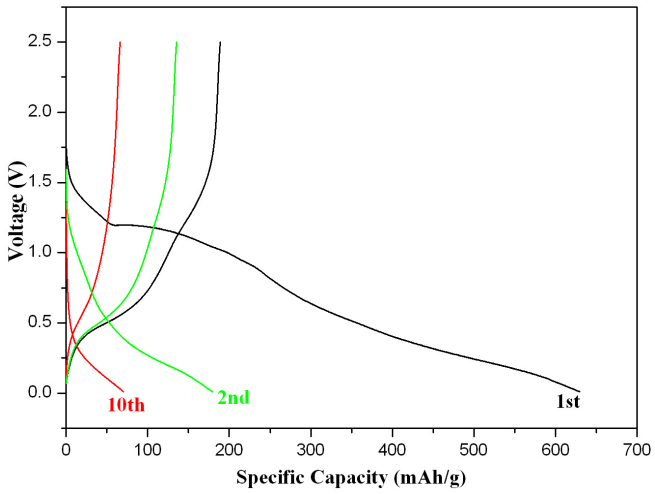

Figure 4. Charge/discharge curves of the TiO_2-SnO_2 nanocomposite at the current density of 40 $mA.g^{-1}$ between 0.01 and 2.5 V.

of the nanocomposite is calculated to be 0.75, which is lower than that of the raw layout (≈0.93) due to a certain amount protonated titanate nanowires loss during washing after the first-step hydrothermal treatment.

Spray-drying technique is a way to prepare nanoparticle granules with a good flowability and a size without inducing additional hard agglomerates, as well as exhibiting advantages like low price, high efficiency. Nakahara et al. reported excellent cycling performance of particulate $Li_4Ti_5O_{12}$ prepared by spray drying process with LiOH and anatase type TiO_2 as precursors, and it was found that granular morphology of the active $Li_4Ti_5O_{12}$ was essential to the high rate capacity of the active materials [33]. In our previous work, porous TiO_2 nanowire microspheres within a size of 2-10 μm were prepared by one-step hydrothermal reaction and subsequent spray drying treatment. Thus, the formation of the donut-like microsphere structure in the as-obtained TiO_2-SnO_2 nanocomposite should be related with both the second-step hydrothermal treatment and spray drying process.

Fig. 4 displays the galvanostatic discharging-charging curves of the as-prepared TiO_2-SnO_2 nanocomposite at a current rate of 40 $mA.g^{-1}$ over the potential range of 0.01-2.5 V (versus Li^+/Li). The initial discharge capacities is 640 $mAh.g^{-1}$, which is much higher than the theoretical capacity of TiO_2(B) but a little lower than

SnO_2. And the charge capacity (charge capacity less than discharge for the anode materials) is 200 mAh.g^{-1}, indicating a large capacity loss during the lithium insertion/extraction in the as-prepared TiO_2-SnO_2 nanocomposite. This irreversible capacity could be caused by the formation of Li_2O, the inevitable formation of solid electrolyte interface and/or the occurrence of some complicated side reactions. The charge specific capacities tend to decrease as cycle number increases, and approximately 11% (70 mAh g^{-1}) of its initial discharge capacity is retained after 10 cycles, showing unsatisfying cycle stability. In these respects, further work is being carried out to improve the lithium storage performance of the donut-like TiO_2-SnO_2 microspheres.

4. CONCLUSION

In summary, TiO_2-SnO_2 nanocomposite was first prepared on a large scale by a two-step hydrothermal reaction followed by spray drying and post-heat treatment. The hierarchical donut-like TiO_2-SnO_2 microspheres within a size of 1-5 μm were achieved by the second-step hydrothermal treatment and subsequent spray drying. The transformation from TiO_2(B) into anatase TiO_2 phase at relatively high temperature was hampered because of the high interaction between TiO_2 and SnO_2, which also resulted in the formation of the substitutional solid solution (Sn, Ti)O_2 with the same tetragonal rutile structure as SnO_2. The as-obtained donut-like TiO_2-SnO_2 nanocomposite microspheres demonstrated a high initial discharge capacity as anode materials for lithium-ion batteries, implying a promising anode candidate for lithium-ion batteries if the coulombic efficiency could be improved.

5. ACKNOWLEDGMENT

This work was financially supported by the Zhejiang Analysis Test Project of China (2009F70010, 2012C37068) and the National Natural Science Foundation of China (21003111, 21210102012).

REFERENCES

[1] H.Bin Wu, J.S. Chen, H.H. Hong, X.W. Lou, Nanoscale, 4, 2526 (2012).

[2] L. Kavan, M. Gratzel, J. Rathousky, A. Zukal, J. Electrochem. Soc., 143, 394 (1996).

[3] H. Lindstrom, S. Sodergren, A. Solbrand, H. Rensmo, J. Hjelm, A. Hagfeldt, S.E. Lindquist, J. Phys. Chem., B, 101, 7717 (1997).

[4] R.van de Krol, A. Goossens, E.A. Meulenkamp, J. Electrochem. Soc., 146, 3150 (1990).

[5] M. Wagemaker, G.J. Kearley, A.A.van Well, H. Mutka, F.M. Mulder, J. Am. Chem. Soc., 125, 840 (2003).

[6] J.S. Chen, X.W. Lou, J. Power Sources, 195, 2905 (2010).

[7] M. Pfanzelt, P. Kubiak, M. Fleischhammer, M. Wohlfahrt-Mehrens, J. Power Sources, 196, 6815 (2011).

[8] D. Dambournet, I. Belharouak, K. Amine, Chem. Mater., 22, 1173 (2010).

[9] A.R. Armstrong, G. Armstrong, J. Canales, P.G. Bruce, Angew. Chem. Int. Ed., 43, 2286 (2004).

[10]A.R. Armstrong, G. Armstrong, J. Canales, R. Garcia, P.G. Bruce, Adv. Mater., 17, 862 (2005).

[11]G. Armstrong, A.R. Armstrong, J. Canales, P.G. Bruce, Chem. Commun., 19, 2454 (2005).

[12]A.R. Armstrong, G. Armstrong, J. Canales, P.G. Bruce, J. Power Sources, 146, 501 (2005).

[13]S.H. Liu, H.P. Jia, L. Han, J.L. Wang, P.F. Gao, D.D. Xu, J. Yang, S.N. Che, Adv. Mater., 24, 3201 (2012).

[14]Q.J. Li, J.W. Zhang, B.B. Liu, M. Li, R. Liu, X.L. Li, H.L. Ma, S.D. Yu, L. Wang, Y.G. Zou, Z.P. Li, B. Zou, T. Cui, G.T Zou, Inorg. Chem., 47, 9870 (2008).

[15]Q.L. Wu, J.C. Li, R.D. Deshpande, N. Subramanian, S.E. Rankin, F.Q Yang, Y.T. Cheng, J. Phys. Chem. C, 116, 18669 (2012).

[16]S.M. Dong, H.B. Wang, L. Gu, X.H. Zhou, Z.H. Liu, P.X. Han, Y. Wang, X. Chen, G.L. Cui, L.Q. Chen, Thin Solid Films, 519, 5978 (2011).

[17]J.S. Chen, Y.L. Tan, C.M. Li, Y.L. Cheah, D.Y. Luan, S. Madhavi, F.Y.C. Boey, L.A. Archer, X.W. Lou, J. Am. Chem. Soc., 132, 6124 (2010).

[18]J.F. Ye, W. Liu, J.G. Cai, S. Chen, X.W. Zhao, H.H. Zhou, L.M. Qi, J. Am. Chem. Soc., 133, 933 (2011).

[19]H.E. Wang, H. Cheng, C.P. Liu, X. Chen, Q.L. Jiang, Z.G. Lu, Y.Y. Li, C.Y. Chung, W.J. Zhang, J.A. Zapien, L. Martinu, I. Bello, J. Power Sources, 196, 6394 (2011).

[20]D. Larcher, S. Beattie, M. Morcrette, K. Edstroem, J.C. Jumas, J.M. Tarascon, J. Mater. Chem., 17, 3759 (2007).

[21]J.S. Chen, Y.L. Cheah, Y.T. Chen, N. Jayaprakash, S. Madhavi, Y.H. Yang, X.W. Lou, J. Phys. Chem. C, 113, 20504 (2009).

[22]J.S. Chen, L.A. Archer, X.W. Lou, J. Mater. Chem., 21, 9912 (2011).

[23]X.W. Lou, Y. Wang, C.L. Yuan, J.Y. Lee, L.A. Archer, Adv. Mater., 18, 2325 (2006).

[24]X.W. Lou, C.M. Li, L.A. Archer, Adv. Mater., 21, 2536 (2009).

[25]X.W. Lou, J.S. Chen, P. Chen, L.A. Archer, Chem. Mater., 21, 2868 (2009).

[26]S.Y. Vassiliev, A.I. Yusipovich, Y.E. Rogynskaya, F.K. Chibirova, A.M. Skundin, T.L. Kulova, J. Solid State Electrochem., 9, 698 (2005).

[27]J. Jamnik, R. Dominko, B. Erjavec, M. Remskar, A. Pintar, M. Gaberscek, Adv. Mater., 21, 2715 (2009).

[28]Z.X. Yang, G.D. Du, Q. Meng, Z.P. Guo, X.B. Yu, Z.X. Chen, T.L. Guo, R. Zeng, RSC Adv., 1, 1834 (2011).

[29]Y.M. Lin, R.K. Nagarale, K.C. Klavetter, A. Heller, C. Buddie Mullins, J. Mater. Chem., 22, 11134 (2012).

[30]X.M. Wu, S.C. Zhang, L.L. Wang, Z.J. Du, H. Fang, Y.H. Ling, Z.H. Huang, J. Mater. Chem., 22, 11151 (2012).

[31]S.J. Ding, J.S. Chen, X.W. Lou, Adv. Funct. Mater, 21, 4120 (2011).

[32]Y.F. Wang, M.Y. Wu, W.F. Zhang, Electrochimica Acta, 53, 7863 (2008).

[33]K. Nakahara, R. Nakajima, T. Matsushima, H. Majima, J. Power Sources, 117, 131 (2003).